

DOI: 10.1002/cbic.200800005

Arginine Dynamics in a Membrane-Bound Cationic Beta-Hairpin Peptide from Solid-State NMR

Ming Tang,^[a] Alan J. Waring,^[b] and Mei Hong^{*[a]}

The site-specific motion of Arg residues in a membrane-bound disulfide-linked antimicrobial peptide, protegrin-1 (PG-1), was investigated by using magic-angle-spinning solid-state NMR spectroscopy to better understand the membrane insertion and lipid interaction of this cationic membrane-disruptive peptide. The C–H and N–H dipolar couplings and ¹³C chemical shift anisotropies were measured in the anionic POPE/POPG membrane, and were found to be reduced from the rigid-limit values by varying extents; this indicates the presence of segmental motion. An Arg residue at the β -turn region of the peptide showed much weaker spin interactions, which indicates larger amplitudes of motion than an Arg residue in the β -strand region of the peptide. This is

consistent with the exposure of the β turn to the membrane surface and the immersion of the β strand in the hydrophobic middle of the membrane, and supports the previously proposed oligomerization of the peptide into β barrels in the anionic membrane. The ¹³C T₂ and ¹H T_{1 ρ} relaxation times indicate that the β -turn backbone undergoes large-amplitude intermediate-timescale motion in the fluid phase of the membrane; this causes significant line broadening and loss of spectral intensity. This study illustrates the strong correlation between the dynamics and structure of membrane proteins, and the capability of solid-state NMR spectroscopy to provide detailed information on site-specific dynamics in complex membrane-protein assemblies.

Introduction

Molecular motion is common in membrane proteins and is often intimately related to the function and lipid interaction of these molecules. Solid-state NMR (SSNMR) spectroscopy is a versatile tool for characterizing molecular dynamics on a wide range of timescales (picoseconds to seconds), and for determining the amplitude of anisotropic motion. Large-amplitude segmental motion has been reported, for example, for a bacterial toxin that spontaneously inserts into the lipid membrane as a result of its intrinsic conformational plasticity,^[1] a lipidated Ras signaling protein,^[2] the catalytic domain of a membrane-bound enzyme,^[3] and the loops of the seven-transmembrane-helix protein rhodopsin.^[4] In addition to internal segmental motion, whole-body reorientation has been discovered for many small membrane peptides of both β -sheet and α -helical secondary structures.^[5–7]

Protegrin-1 (PG-1) is a broad-spectrum antimicrobial peptide found in porcine leukocytes.^[8,9] It is a β -hairpin molecule that is stabilized by two disulfide bonds and contains six Arg residues (RGGRLCYCRRRFCVCVGR). PG-1 achieves its antimicrobial function by forming nonselective pores in the microbial cell membrane that disrupt the membrane's barrier function.^[10,11] Recently, the high-resolution oligomeric structure of PG-1 at these pores was determined by using ¹H and ¹⁹F spin-diffusion NMR spectroscopic techniques.^[12] The peptide was found to self-assemble into a transmembrane β barrel in bacteria-mimetic anionic POPE/POPG membranes. The ¹³C–³¹P distance constraints indicate that the Arg residues in these transmembrane β barrels are complexed with lipid phosphates;^[13] this suggests that charge neutralization by ion pairing reduces the free energy of peptide insertion into the hydrophobic part of the

membrane, and the consequent tethering of lipid headgroups might be the cause for toroidal pore formation.

The experiments that yielded the equilibrium oligomeric structure of PG-1 and the toroidal pore morphology of the lipid membrane were carried out at low temperatures of about –40 °C, which is in the gel phase of the membrane, to eliminate any motion that would average the distance-dependent dipolar couplings. On the other hand, PG-1 carries out its antimicrobial action in the liquid-crystalline (LC) phase of the membrane, where it is expected to be more mobile. How the dynamics of PG-1 and its Arg side chains affect toroidal pore formation has not yet been studied. If Arg–phosphate complex formation is true, then the functional groups involved in the complex, that is, the guanidinium ions, the lipid phosphates, and possibly water, should be less mobile than in their respective bulk environments. Thus, understanding Arg motion in PG-1 in the lipid membrane might provide additional insight into guanidinium–phosphate interaction. More generally, although the motion of long-chain amino-acid residues has begun to be investigated in microcrystalline proteins,^[14–16] motion of the same residues in membrane proteins is still scarcely studied by NMR spectroscopy. Arg is particularly

[a] M. Tang, Prof. M. Hong
Department of Chemistry, Iowa State University
Ames, IA 50011 (USA)
Fax: (+1) 515-294-0105
E-mail: mhong@iastate.edu

[b] Prof. A. J. Waring
Department of Medicine
University of California at Los Angeles School of Medicine
Los Angeles, CA 90095 (USA)

common in many medically important membrane peptides and proteins such as antimicrobial peptides (AMPs),^[17] cell-penetrating peptides,^[18,19] and voltage-sensing domains of ion channels.^[20]

In this work we report the amplitudes of the microsecond timescale motions of Arg and other residues in PG-1 that are bound to the POPE/POPG membrane. We found that an Arg in the β -strand part of the molecule, which is embedded in the hydrophobic interior of the membrane is much less mobile than an Arg in the β -turn part of the molecule, which is exposed to the membrane surface. This is consistent with the oligomeric structure and lipid interaction of this antimicrobial peptide.

Results

We first characterized the dynamic structure of PG-1 in POPE/POPG bilayers by variable-temperature ^{13}C and ^{15}N CP-MAS NMR spectroscopy experiments. A series of CP spectra were collected between 243 and 308 K on PG-1 that contained U- ^{13}C , ^{15}N -labeled Arg4, Leu5, and Arg11, and ^{15}N -labeled Phe12. As shown in Figure 1, the $\text{C}\alpha$ peaks of Arg4 and Leu5 are much sharper and higher than the $\text{C}\alpha$ peak of Arg11. At 295 K, the full widths at half-maximum (FWHM) of Arg4 and Leu5 $\text{C}\alpha$'s were ~ 3 ppm, compared to 6 ppm for the Arg11 $\text{C}\alpha$. As the temperature decreases, the Arg11 $\text{C}\alpha$ intensity increases

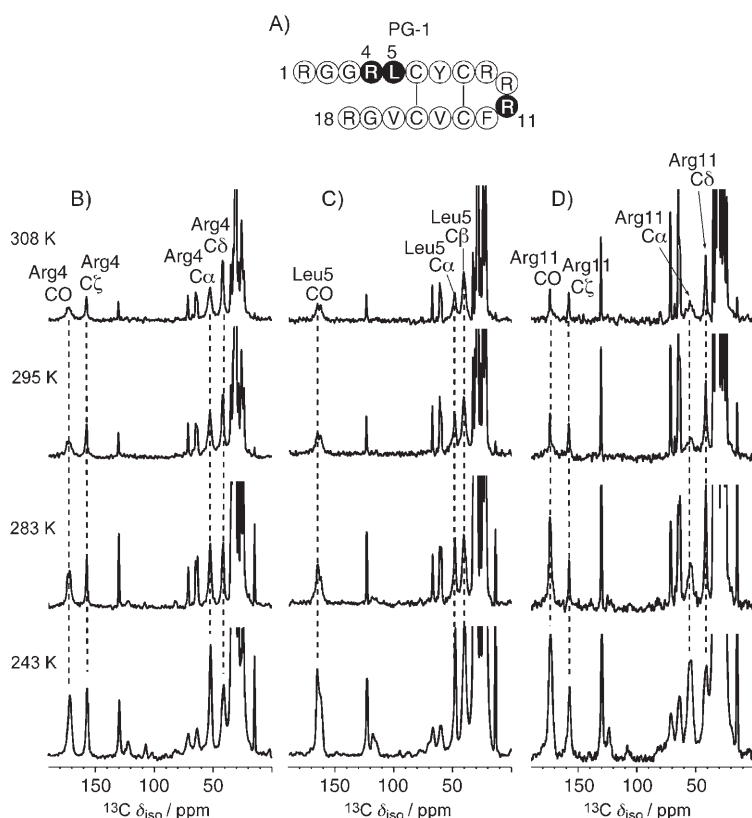


Figure 1. ^{13}C CP-MAS NMR spectra in PG-1 bound to the POPE/POPG membrane (P/L, 1:1.25) from 243 to 308 K. A) Amino acid sequence of PG-1; labeled residues are shaded. B) ^{13}C CP-MAS NMR spectra of Arg4; C) ^{13}C CP-MAS NMR spectra of Leu5; D) ^{13}C CP-MAS NMR spectra of Arg11. Peptide peaks are assigned and annotated.

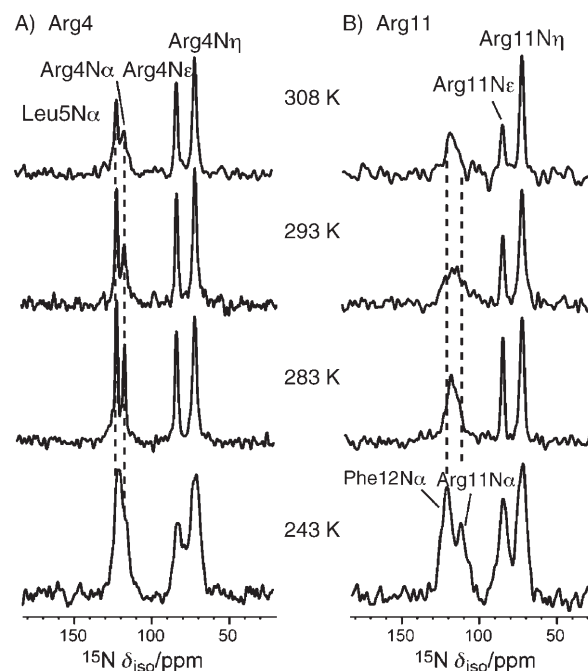


Figure 2. ^{15}N CP-MAS NMR spectra of PG-1 in the POPE/POPG membrane at various temperatures. A) Arg4, Leu5; B) Arg11 and Phe12. Assignments were obtained from the 2D ^{13}C - ^{15}N NMR correlation spectra (not shown).

significantly. This suggests that in the liquid-crystalline phase of the membrane the Arg11 backbone undergoes large-amplitude intermediate-timescale motion that becomes frozen in the gel phase of the membrane, while the Arg4 and Leu5 $\text{C}\alpha$ sites are more rigid. In other words, the β -turn backbone is more mobile than the β -strand backbone. A similar trend is observed in the ^{15}N CP-MAS NMR spectra (Figure 2). The backbone $\text{N}\alpha$ peaks of Arg4 and Leu5 are sharp and well resolved, with FWHM of 2–3 ppm at 283 K, but the Arg11 $\text{N}\alpha$ peak is broad and overlaps with Phe12 $\text{N}\alpha$ to give a FWHM of 9 ppm for the combined peak at 283 K. Only at 243 K do the Arg11 $\text{N}\alpha$ and Phe12 $\text{N}\alpha$ peaks become resolved. We assigned the $\text{N}\alpha$ peaks by ^{13}C - ^{15}N 2D NMR spectroscopic correlation experiments (data not shown).^[21]

To distinguish between the contribution of the static structural heterogeneity versus dynamic disorder to the linewidths, we measured the ^{13}C T_2 relaxation times of Arg4 and Arg11 at two different temperatures, 283 and 243 K, by using the Hahn echo experiment. Table 1 shows the ^{13}C apparent linewidths, Δ^* , which were read off from the CP spectra, and the ^{13}C homogeneous linewidths, Δ , which were obtained from the T_2 values according to $\Delta = 1/\pi T_2$. At 243 K, the homogeneous linewidths of Arg4 and Arg11 are similar; this indicates that the motion is largely frozen. However, the apparent linewidth of the Arg11 backbone $\text{C}\alpha$ (604 Hz, or 6.0 ppm) is much larger than Arg4 $\text{C}\alpha$ (222 Hz, or 2.2 ppm); this indicates that there is much more conformational disorder

Table 1. ^{13}C apparent linewidths (Δ^*) and homogeneous linewidths (Δ) of PG-1 in POPE/POPG membrane at 283 and 243 K. The apparent linewidths were read off from 1D CP spectra. The homogeneous linewidths were obtained from T_2 measurements as $\Delta = 1/\pi T_2$. The linewidths were measured at a ^{13}C Larmor frequency of 100 MHz.

Residue	Sites	283 K		243 K	
		Δ^* [Hz]	Δ [Hz]	Δ^* [Hz]	Δ [Hz]
Arg4	C α	272	199	222	118
	C δ	222	187	493	289
	C ζ	111	84	201	80
Arg11	C α	473	289	604	133
	C δ	161	106	534	265
	C ζ	81	53	222	94

der at the β -turn backbone than at the β strand. In comparison, the side chains of Arg4 and Arg11 at 243 K exhibit similar homogeneous linewidths as well as similar apparent linewidths; this indicates that both the static and dynamic heterogeneities are comparable for the two side-chains. At 283 K, the Arg11 C α exhibits both larger Δ and larger Δ^* than the Arg4 C α ; this indicates that the β -turn backbone has greater dynamic as well as static disorder than the β -strand backbone. In contrast, the side-chain of Arg11 has narrower Δ and Δ^* than the Arg4 side-chain; this indicates that the Arg11 side-chain undergoes faster motions than the Arg4 side-chain.

To obtain information on the motional amplitudes of the Arg side-chains, especially the guanidinium group, we measured the ^{13}C chemical shift anisotropy (CSA) of C ζ , the center of the guanidinium ion. We chose the intermediate temperature of 283 K for the CSA and the subsequent dipolar coupling experiments since at this temperature the spectra have the best overall combination of resolution and sensitivity. The theoretical phase-transition temperature of the POPE/POPG (3:1) membrane is 291 K, thus the spectra theoretically correspond to the gel-phase membrane, but the phase transition is likely broadened by the peptide. The peptide mobility closer to the physiological temperature can be extrapolated from the 283 K data and is expected to be higher, but the differences between residues should be similar. We used the 2D separation of undistorted powder patterns by the effortless recoupling (SUPER) experiment^[22] to recouple the CSA interaction and correlate it with the isotropic ^{13}C chemical shift. Figure 3 shows the 2D SUPER spectra and 1D cross sections of the model compound Fmoc-Arg(MTR)-OH, and Arg4 and Arg11 in PG-1 bound to the POPE/POPG membrane. For the dry powder sample of Fmoc-Arg(MTR)-OH, the C ζ cross section yielded a CSA anisotropy parameter δ , which is defined as the difference between the largest principal value δ_{zz} and the isotropic shift δ_{iso} of 78 ppm. This CSA is the rigid-limit value, since C–H dipolar couplings of the side-chain carbons in this model compound have nearly rigid-limit values (Table 2). In comparison, the C ζ of Arg4 and Arg11 of PG-1 both give reduced CSAs: the Arg4 C ζ δ is 47.3 ppm whereas the Arg11 C ζ CSA is much smaller at 10.3 ppm. These correspond to a motional scaling factor of 0.13 for Arg11 and 0.61 for Arg4. Thus, the Arg11 side-chain has larger amplitude motion than Arg4. Since the T_2 data indi-

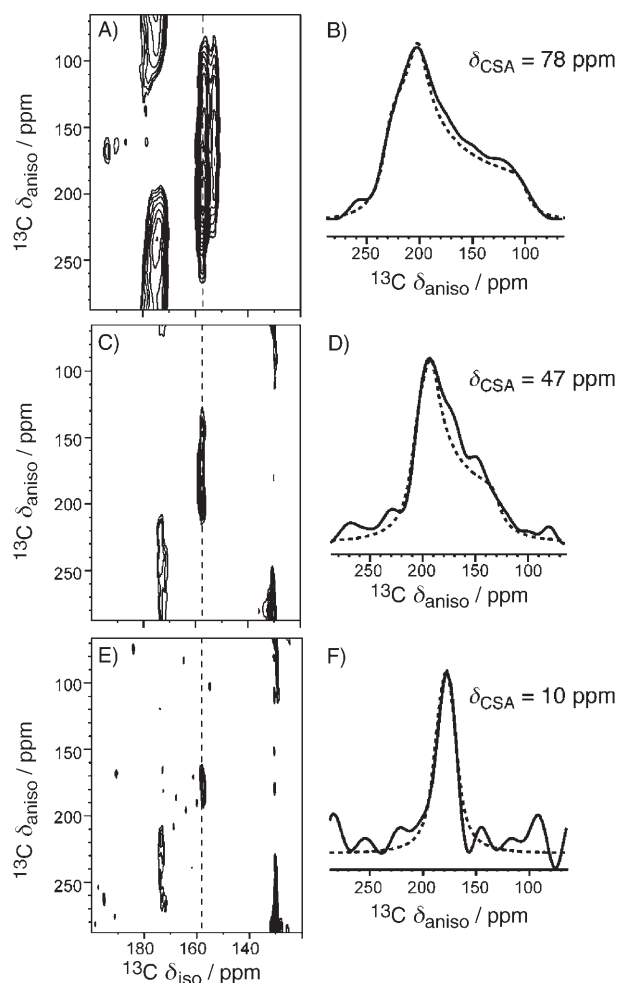


Figure 3. Arg C ζ chemical-shift anisotropies from the SUPER experiment. The 2D SUPER spectra are shown in A), C), E), and the corresponding C ζ 1D cross sections are shown in B), D), and F). A) and B) Fmoc-Arg(MTR)-OH. C) and D) PG-1 Arg4. E) F) PG-1 Arg11. The PG-1 data were measured at 283 K in the POPE/POPG membrane.

Table 2. Dipolar order parameters and CSA motional scaling factors^[a] of PG-1 residues at 283 K and of three crystalline model compounds at 295 K.

Sites	Arg4	Arg11	Fmoc-Arg	Arg-HCl	Leu5	Leu
N α	1.05	0.70	–	–	0.95	–
C α	0.93	0.70	0.91	0.91	0.93	0.95
C β	0.61	–	0.86	0.91	0.56	0.93
C γ	0.63	–	0.91	0.91	0.44	–
C δ	0.48	0.21	0.91	1.02	0.43	0.34
N ϵ	0.48	0.24	–	–	–	–
C ζ ^[a]	0.61	0.13	–	–	–	–
N η	0.36	0.28	–	–	–	–

cate narrower homogeneous linewidths of Arg11 C δ and C ζ than Arg4, the Arg11 side-chain motion is both faster and larger in amplitude than the Arg4 side-chain motion.

To obtain more quantitative information on the motional amplitude, we measured C–H and N–H dipolar couplings, whose tensor orientation and rigid-limit coupling strength are

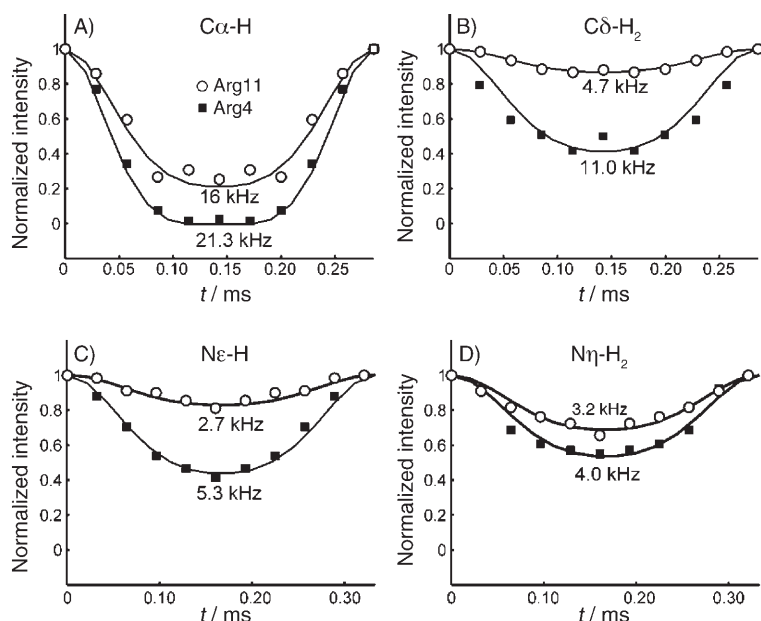


Figure 4. ^{13}C - ^1H and ^{15}N - ^1H DIPSHIFT curves of several sites of Arg4 (■) and Arg11 (○) in PG-1 at 283 K. A) $\text{C}\alpha$ -H; B) $\text{C}\delta$ - H_2 ; C) $\text{N}\epsilon$ -H; D) $\text{N}\eta$ - H_2 . Arg11 gives weaker couplings than Arg4; this indicates larger motional amplitudes.

exactly known. The dipolar couplings were readily measured by using the 2D dipolar chemical shift correlation (DIPSHIFT) experiment to yield the bond order parameter, $S = \bar{\delta}/\delta$. Figure 4 shows representative DIPSHIFT curves of Arg4 and Arg11 in POPE/POPG-bound PG-1. $\text{C}\alpha$ -H represents the backbone, while $\text{C}\delta$ - H_2 , $\text{N}\epsilon$ -H, and $\text{N}\eta$ - H_2 represent the side-chains. The order parameters are compiled in Table 2. Both the backbone $\text{N}\alpha$ and $\text{C}\alpha$ of Arg4 and Leu5 exhibited nearly rigid-limit couplings, with order parameters of 0.93–1.00. In contrast, the Arg11 $\text{C}\alpha$ and $\text{N}\alpha$ have significantly lower order parameters of 0.70. Thus, the β -strand backbone of the peptide is immobilized in the POPE/POPG membrane at this temperature, whereas the Arg11 backbone retains significant local segmental motion. For resolved sites ($\text{C}\delta$, $\text{N}\epsilon$, and $\text{N}\eta$) in the side chains, Arg4 and Leu5 also have stronger dipolar couplings than those of Arg11; this indicates that the β -strand side chains have smaller amplitudes of motion, which is consistent with the variable-temperature spectra and the CSA results. Some ^{13}C sites in the side-chain, such as Arg $\text{C}\beta$, $\text{C}\gamma$, Leu $\text{C}\gamma$, and $\text{C}\delta$, overlap with the

lipid peaks, so we used a double-quantum (DQ) filtered DIPSHIFT experiment to suppress the lipid signals and measure the C-H couplings of these Arg sites.^[1] Figure 5 shows representative 1D DQ NMR spectra and DQ-DIPSHIFT dephasing curves of Arg4 and Leu5. Arg11 has prohibitively low sensitivity in the DQ-DIPSHIFT experiment due to unfavorable motional rates at this temperature, and was thus not measured. Table 2 shows that in general the side-chain order parameters decrease with increasing distance from the backbone. Arg11 at the β turn, which is close to the membrane surface, has much higher amplitudes of motion, or much lower order parameters, than Arg4 and Leu5 in the β -strand part of the peptide, which is embedded in the membrane.^[12]

To obtain further information on the rates of motions of these residues, we measured the ^1H $T_{1\rho}$ relaxation times (Table 3). Most sites in Arg4, Leu5, and Arg11 have similar ^1H $T_{1\rho}$ values (1.6–2.6 ms), except for Arg11 $\text{H}\alpha$, which has a much shorter $T_{1\rho}$ (0.83 ms) than Arg4 $\text{H}\alpha$ (2 ms). This is consistent with the ^{13}C T_2 data that indicates more pronounced intermediate-timescale motion of the β -turn backbone compared to the β -strand backbone.

Discussion

The solid-state NMR spectroscopy data shown here indicate that the β -turn backbone of PG-1 undergoes large-amplitude segmental motion on the microsecond timescale, whereas the β -strand backbone is mostly immobilized in the POPE/POPG

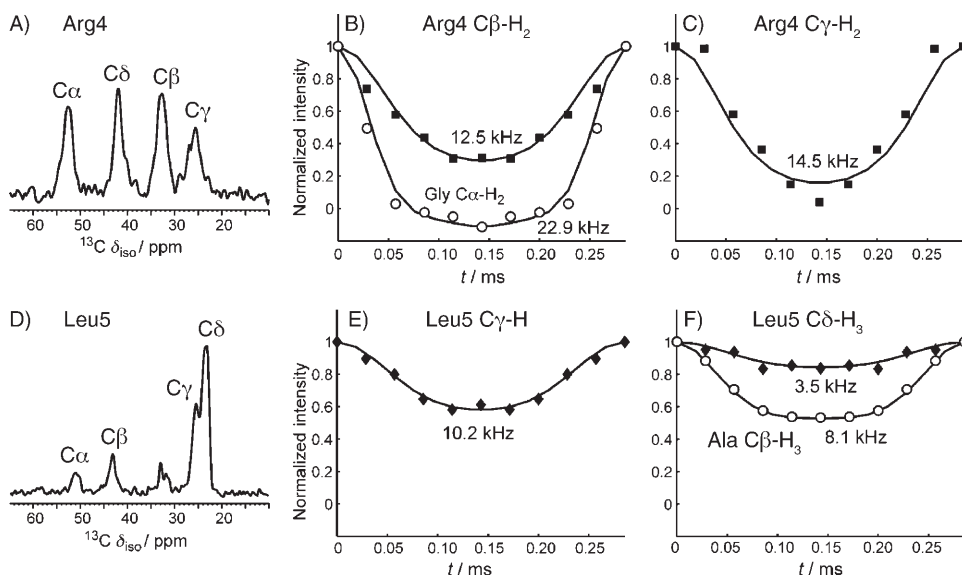


Figure 5. 1D ^{13}C DQ NMR filtered spectra and DQ-DIPSHIFT curves of Arg4 and Leu5 in PG-1 in the POPE/POPG membrane. A) 1D ^{13}C DQ NMR spectrum of Arg4. The $\text{C}\beta$ and $\text{C}\gamma$ peaks no longer overlap with the lipid peaks. B) DIPSHIFT curves of Arg4 $\text{C}\beta$ (■) and the crystalline amino acid Gly $\text{C}\alpha$ (○). The Gly $\text{C}\alpha$ data give the rigid-limit coupling for CH_2 groups, which is 22.9 kHz. C) DIPSHIFT curve of Arg4 $\text{C}\gamma$. D) 1D DQ spectrum of Leu5. The $\text{C}\gamma$ and $\text{C}\delta$ peaks no longer overlap with the lipid peaks. E) DIPSHIFT curve of Leu5 $\text{C}\gamma$. F) DIPSHIFT curves of Leu5 $\text{C}\delta$ (◆) and the crystalline amino acid Ala $\text{C}\beta$ (○). The Ala $\text{C}\beta$ data give the rigid-limit coupling for methyl groups, which is 8.1 kHz. This is one-third of the one bond C-H coupling due to the three-site jump of the CH_3 group.

Table 3. ^1H $T_{1\rho}$ [ms] of POPE/POPG-bound PG-1 at 283 K and of crystalline Arg-HCl at 295 K. Experimental uncertainties are given in parentheses. The ^1H spin-lock field strengths were 50 kHz in the ^{15}N -detected experiment and 62.5 kHz in the ^{13}C -detected experiments.

Sites	Arg4	Arg11	Arg-HCl
H ^N	2.6 (0.2)	2.2 (0.3)	–
H α	2.0 (0.1)	0.8 (0.1)	8.8
H δ	1.6 (0.1)	1.9 (0.1)	9.5
H ϵ	2.2 (0.2)	2.6 (0.2)	8.8
H η	1.9 (0.2)	1.8 (0.1)	8.8

membrane in the liquid-crystalline phase. The latter is consistent with the previously reported immobilization of PG-1 strand residues in POPC/POPG membranes.^[23] Concomitant with the backbone mobility difference, the side-chains also exhibit dynamic differences: Arg11 has much lower order parameters than Arg4 (Table 2); consistent with large motional amplitudes. Both membrane-associated Arg residues are much more mobile than the crystalline compound Arg-HCl.

The dynamic difference between Arg4 and Arg11 can be understood in terms of the self-assembly of PG-1 and the peptide-lipid interactions. The β strands that contain Arg4 and Leu5 are involved in intermolecular association with other PG-1 molecules through N–H...O=C hydrogen bonds to form β barrels,^[12,24] thus these residues should experience hindered motion. The strand aggregation is important to PG-1's antimicrobial activity. Mutation of Val14 to *N*-methyl-Val, which disrupted hydrogen bonding of the Val14 backbone to its intermolecular partner, resulted in much lower antimicrobial activity.^[25] In contrast, the β -turn Arg11 is not involved in intermolecular hydrogen bonding, and is located near the membrane surface, thus it has more motional freedom.

A second contributing factor to the different side-chain dynamics of Arg11 and Arg4 might be the guanidinium–phosphate interaction. The ^{13}C – ^{31}P spectroscopic distance data indicated that both side-chains lie within hydrogen-bonding distance to lipid phosphates.^[13] However, while the Arg4 guanidinium group interacts with the phosphate groups that have moved to the middle of the membrane as part of the toroidal pore, the Arg11 guanidinium ion interacts with phosphates at the membrane surface with much higher mobility. Thus, the motional restriction caused by the lipid phosphate groups is more severe for Arg4 than for Arg11. We note that at the temperature of 283 K, at which most dynamic data were obtained, the lipid molecules were much more mobile than at \sim 230 K, at which the ^{13}C – ^{31}P distances were measured. Thus, the guanidinium–phosphate association at 283 K is likely to be transient rather than permanent.

The high mobility of the β -hairpin tip of PG-1 dovetails the observation of an analogous β -hairpin antimicrobial peptide, TP-1.^[26] In TP-1, Gly10 at the β turn exhibited an order of magnitude shorter ^1H $T_{1\rho}$ relaxation times than the β -strand residues. Field-dependent $T_{1\rho}$ analysis indicated that the shorter $T_{1\rho}$ of Gly10 is a result of larger motional amplitudes of the β turn and not because of rate differences from the rest of the peptide.^[26]

Molecular dynamics simulations of the S4 helix of the voltage-gated potassium channel KvAP^[27] suggested that lipid headgroups and water stabilize Arg insertion by forming a hydrogen-bonded network. The effective lipid bilayer thickness was reduced to a remarkably small 10 Å near the inserted S4 helix so that water and phosphate groups can stabilize the Arg residues in the middle of the S4 helix by hydrogen bonds.^[28] Based on the comparison of the mean-square displacement of phosphate groups near the peptide with those far away from the peptide and the analysis of the survival function of water molecules in the system, it was found that both phosphate groups and water molecules are much less mobile in the vicinity of the guanidinium groups than in their respective bulk environments. In particular, the mean residence times for water molecules that are hydrogen-bonded to Arg9 and Arg12 in the S4 helix, which are close to the bilayer surface, are much shorter than those that are hydrogen-bonded to Arg15 and Arg18, which lie in the hydrophobic core of the membrane (90–300 ps vs. 1000–2000 ps). This different residence time suggests that the water molecules near Arg in the hydrophobic core are less mobile than those near Arg at the membrane surface. This in turn suggests that Arg residues in the hydrophobic part of the membrane are less mobile than those close to the bilayer surface. These are consistent with the different mobility that is observed between Arg4 and Arg11 in PG-1.

In summary, we have measured the dipolar couplings, CSAs, and T_2 and $T_{1\rho}$ relaxation times of key Arg residues in PG-1 in the bacteria-mimetic anionic POPE/POPG membrane. The linewidths and motional scaling factors show that the β -turn Arg11 near the membrane surface is significantly more mobile than the β -strand Arg4 and Leu5 in the hydrophobic part of the membrane. The different mobility is consistent with the location of the residues with respect to the membrane, the intermolecular aggregation of PG-1, and the strong Arg-phosphate interaction. Thus, the site-specific dynamics of PG-1 correlate well with its topological and oligomeric structure. Solid-state NMR is shown to be a useful tool for elucidating the relation between membrane protein dynamics and its structure.

Experimental Section

1-Palmitoyl-2-oleoyl-*sn*-glycero-3-phosphatidylethanolamine (POPE), and 1-palmitoyl-2-oleoyl-*sn*-glycero-3-phosphatidylglycerol (POPG) were purchased from Avanti Polar Lipids (Alabaster, AL, USA). PG-1 (NH₂-RGGRLCYRRRFCVCGR-CONH₂) was synthesized by using Fmoc chemistry as previously described.^[7] Three PG-1 samples were synthesized that contained U- ^{13}C , ^{15}N -Arg4, and ^{15}N -Leu5, U- ^{13}C , ^{15}N -Arg11, and ^{15}N -Phe12, U- ^{13}C , ^{15}N -Leu5. U- ^{13}C , ^{15}N -labeled Arg was obtained from Spectra Stable Isotopes (Columbia, MD, USA) as Fmoc-Arg(MTR)-OH.

POPE and POPG lipids (3:1) were mixed in CHCl₃ and blown dry under N₂ gas. The mixture was then redissolved in cyclohexane and lyophilized. The dry lipid powder was dissolved in H₂O and subjected to five cycles of freeze-thawing to form uniform vesicles. An appropriate amount of PG-1 for a peptide–lipid molar ratio (P/L) of 1:12.5 was dissolved in H₂O and mixed with the lipid vesicle solution, incubated at 303 K overnight, then centrifuged at

55 000 rpm for 2.5 h. The pellet was packed into a MAS rotor to give a fully hydrated membrane sample.

NMR spectroscopy experiments were carried out by using a Bruker DSX 400 (9.4 Tesla) spectrometer (Karlsruhe, Germany). Triple-resonance magic-angle spinning (MAS) probes with a 4 mm spinning module were used. Temperatures were controlled by a Kinetics Thermal Systems XR air-jet sample cooler (Stone Ridge, NY, USA) on the 400 MHz system. Typical 90° pulse lengths were 5–6 μs for ¹³C and ¹⁵N, and ¹H decoupling fields of 50–80 kHz were used. The ¹³C chemical shifts were referenced externally to the α-Gly ¹³C' signal at 176.49 ppm on the tetramethylsilane scale. The ¹⁵N chemical shifts were referenced externally to the *N*-acetyl-Val ¹⁵Nα signal at 121.72 ppm.

¹³C–¹H and ¹⁵N–¹H dipolar couplings were measured by using the 2D DIPSHIFT experiment at 3.0–3.5 kHz MAS with MREV-8 for ¹H homonuclear decoupling.^[29] Pulse lengths of 3.5 μs were used in the MREV-8 pulse train. The N–H DIPSHIFT experiments were performed with dipolar doubling to increase the precision of the measured couplings.^[30,31] Some ¹³C sites overlap with lipid peaks, so the double-quantum-filtered (DQ) DIPSHIFT experiments were used to measure these dipolar couplings.^[1] The DQ filter used SPC5 homonuclear dipolar recoupling sequence.^[32] The ¹³C CSA was measured by using the 2D SUPER experiment under 3.5 kHz MAS.^[22] The corresponding ¹³C field strength was 42 kHz. ¹H rotating-frame spin-lattice relaxation times (*T*_{1ρ}) were measured by using spin-lock field strengths of 50–62.5 kHz. The 1D ¹³C and ¹⁵N NMR spectra were measured between 243 and 308 K. All DIPSHIFT, SUPER and *T*_{1ρ} NMR spectroscopy experiments were carried out at 283 K.

Acknowledgement

This work is supported by the National Institutes of Health grant GM-066976 to M.H.

Keywords: antimicrobial peptides · guanidinium–phosphate complexation · membrane proteins · NMR spectroscopy · order parameters

- [1] D. Huster, L. S. Xiao, M. Hong, *Biochemistry* **2001**, *40*, 7662–7674.
- [2] G. Reuther, K. T. Tan, A. Vogel, C. Nowak, K. Arnold, J. Kuhlmann, H. Waldmann, D. Huster, *J. Am. Chem. Soc.* **2006**, *128*, 13840–13846.
- [3] J. C. Williams, A. E. McDermott, *Biochemistry* **1995**, *34*, 8309–8319.
- [4] M. Eitzkorn, S. Martell, O. C. Andronesi, K. Seidel, M. Engelhard, M. Baldus, *Angew. Chem.* **2007**, *119*, 463–466; *Angew. Chem. Int. Ed.* **2007**, *46*, 459–462.

- [5] S. D. Cady, C. Goodman, W. F. DeGrado, M. Hong, *J. Am. Chem. Soc.* **2007**, *129*, 5719–5729.
- [6] S. H. Park, A. A. Mrse, A. A. Nevzorov, A. A. De Angelis, S. J. Opella, *J. Magn. Reson.* **2006**, *178*, 162–165.
- [7] S. Yamaguchi, T. Hong, A. Waring, R. I. Lehrer, M. Hong, *Biochemistry* **2002**, *41*, 9852–9862.
- [8] L. Bellm, R. I. Lehrer, T. Ganz, *Expert Opin. Invest. Drugs* **2000**, *9*, 1731–1742.
- [9] V. N. Kokryakov, S. S. Harwig, E. A. Panyutich, A. A. Shevchenko, G. M. Aleshina, O. V. Shamova, H. A. Korneva, R. I. Lehrer, *FEBS Lett.* **1993**, *327*, 231–236.
- [10] M. E. Mangoni, A. Aumelas, P. Charnet, C. Roumestand, L. Chiche, E. Despau, G. Grassy, B. Calas, A. Chavanieu, *FEBS Lett.* **1996**, *383*, 93–98.
- [11] Y. Sokolov, T. Mirzabekov, D. W. Martin, R. I. Lehrer, B. L. Kagan, *Biochim. Biophys. Acta Biomembr.* **1999**, *1420*, 23–29.
- [12] R. Mani, S. D. Cady, M. Tang, A. J. Waring, R. I. Lehrer, M. Hong, *Proc. Natl. Acad. Sci. USA* **2006**, *103*, 16242–16247.
- [13] M. Tang, A. J. Waring, M. Hong, *J. Am. Chem. Soc.* **2007**, *129*, 11438–11446.
- [14] J. Lorieau, A. E. McDermott, *Magn. Reson. Chem.* **2006**, *44*, 334–347.
- [15] J. L. Lorieau, A. E. McDermott, *J. Am. Chem. Soc.* **2006**, *128*, 11505–11512.
- [16] B. J. Wylie, W. T. Franks, D. T. Graesser, C. M. Rienstra, *J. Am. Chem. Soc.* **2005**, *127*, 11946–11947.
- [17] R. E. Hancock, R. Lehrer, *Trends Biotechnol.* **1998**, *16*, 82–88.
- [18] E. Vives, P. Brodin, B. Lebleu, *J. Biol. Chem.* **1997**, *272*, 16010–16017.
- [19] P. Jarver, U. Langel, *Biochim. Biophys. Acta Biomembr.* **2006**, *1758*, 260–263.
- [20] S. B. Long, E. B. Campbell, R. Mackinnon, *Science* **2005**, *309*, 897–903.
- [21] M. Hong, R. G. Griffin, *J. Am. Chem. Soc.* **1998**, *120*, 7113–7114.
- [22] S. F. Liu, J. D. Mao, K. Schmidt-Rohr, *J. Magn. Reson.* **2002**, *155*, 15–28.
- [23] J. J. Buffy, A. J. Waring, R. I. Lehrer, M. Hong, *Biochemistry* **2003**, *42*, 13725–13734.
- [24] R. Mani, M. Tang, X. Wu, J. J. Buffy, A. J. Waring, M. A. Sherman, M. Hong, *Biochemistry* **2006**, *45*, 8341–8349.
- [25] J. Chen, T. J. Falla, H. J. Liu, M. A. Hurst, C. A. Fujii, D. A. Mosca, J. R. Embree, D. J. Loury, P. A. Radel, C. C. Chang, L. Gu, J. C. Fiddes, *Biopolymers* **2000**, *55*, 88–98.
- [26] T. Doherty, A. J. Waring, M. Hong, *Biochemistry* **2008**, *47*, 1105–1116.
- [27] T. Hessa, S. H. White, G. von Heijne, *Science* **2005**, *307*, 1427.
- [28] J. A. Freites, D. J. Tobias, G. von Heijne, S. H. White, *Proc. Natl. Acad. Sci. USA* **2005**, *102*, 15059–15064.
- [29] M. G. Munowitz, R. G. Griffin, G. Bodenhausen, T. H. Huang, *J. Am. Chem. Soc.* **1981**, *103*, 2529–2533.
- [30] M. Hong, J. D. Gross, C. M. Rienstra, R. G. Griffin, K. K. Kumashiro, K. Schmidt-Rohr, *J. Magn. Reson.* **1997**, *129*, 85–92.
- [31] D. Huster, S. Yamaguchi, M. Hong, *J. Am. Chem. Soc.* **2000**, *122*, 11320–11327.
- [32] M. Hohwy, C. M. Rienstra, C. P. Jaroniec, R. G. Griffin, *J. Chem. Phys.* **1999**, *110*, 7983–7992.

Received: January 3, 2008

Published online on April 29, 2008